



A self-replication model for long channelized lava flows on the Mars plains

S. M. Baloga¹ and L. S. Glaze^{1,2}

Received 15 June 2007; revised 25 October 2007; accepted 31 January 2008; published 10 May 2008.

[1] A model is presented for channelized lava flows emplaced by a self-replicating, levee-building process over long distances on the plains of Mars. Such flows may exhibit morphologic evidence of stagnation, overflows, and upstream breakouts. However, these processes do not inhibit the formation and persistence of a prominent central channel that can often be traced for more than 100 km. The two central assumptions of the self-replication model are (1) the flow advances at the average upstream velocity of the molten core and (2) the fraction of the lava that travels faster than the average upstream velocity forms stationary margins in the advancing distal zone to preserve the self-replication process. For an exemplary 300 km long flow north of Pavonis Mons, the model indicates that ~ 8 m of crust must have formed during emplacement, as determined from the channel and levee dimensions. When combined with independent thermal dynamic estimates for the crustal growth rate, relatively narrow constraints are obtained for the flow rate ($2250 \text{ m}^3 \text{ s}^{-1}$), emplacement duration (600 d), and the lava viscosity of the molten interior (10^6 Pa s). Minor, transient overflows and breakouts increase the emplacement time by only a factor of 2. The primary difference between the prodigious channelized Martian flows and their smaller terrestrial counterparts is that high volumetric flow rates must have persisted for many hundreds of days on Mars, in contrast to a few hours or days on Earth.

Citation: Baloga, S. M., and L. S. Glaze (2008), A self-replication model for long channelized lava flows on the Mars plains, *J. Geophys. Res.*, 113, E05003, doi:10.1029/2007JE002954.

1. Introduction

[2] The long channelized lava flows on the plains of Mars provide a unique opportunity to develop relatively narrow constraints on emplacement conditions such as viscosity, duration of emplacement, and volumetric flow rate [e.g., Greeley and Crown, 1990; Hodges and Moore, 1994; Zimbelman, 1985; Baloga et al., 2003; Rowland et al., 2004; Glaze and Baloga, 2006; Hiesinger et al., 2007; Garry et al., 2007]. Such flows have prominent well-developed central channels that can often be traced for >100 km (e.g., Figure 1). They have channel widths >5 km, embanking levees of comparable widths, and thicknesses that may exceed 100 m. Flows with these characteristics are found on the plains of Mars where the slopes are typically less than 1° . Detailed examination of the morphologic characteristics of Martian flows suggests complex emplacement mechanisms, including the creation of levees, stagnation of flow advance, overflows, and possibly episodic lava supply [Hodges and Moore, 1994; Mouginitis-Mark and Yoshioka, 1998; Peitersen and Crown, 1999, 2000; Garry et al., 2007].

[3] Emplacement characteristics such as advance rate, volumetric flow rate, and bulk lava viscosity are of direct volcanologic interest and also have implications for subsurface magmatic storage and transport. At present, however, quantitative emplacement characteristics of the long channelized flows on Mars can be constrained to no better than several (or more) orders of magnitude. A fundamental scientific issue that has persisted since the Viking era is whether the large channelized lava flows on Mars even have plausible terrestrial analogs. More specifically, were the Martian flows emplaced by processes and mechanisms known to operate on Earth, or is some uncomfortable or unsupported extrapolation required to explain their characteristics?

[4] The bulk viscosity of the active, deformable fluid component of a long channelized flow on Mars is the primary focus of this work. Viscosity is often used as a single measure of terrestrial lava flow rheology [e.g., Nichols, 1936; Danes, 1972; Pinkerton and Sparks, 1978; Baloga and Pieri, 1986; Glaze and Baloga, 1998; Woodcock and Harris, 2006; Hiesinger et al., 2007; Garry et al., 2007]. In this work, bulk viscosity is defined as the average viscosity of an active, deformable vertical column of fluid lava within the flow. For simplicity, the term “viscosity” will be used in reference to “bulk viscosity” as defined above.

[5] Lava viscosities are strongly controlled by lava temperature, composition, vesicularity, and crystallinity. Terrestrial basalts typically have viscosities in the approximate

¹Proxemy Research, Gaithersburg, Maryland, USA.

²Now at NASA Goddard Space Flight Center, Greenbelt, Maryland, USA.

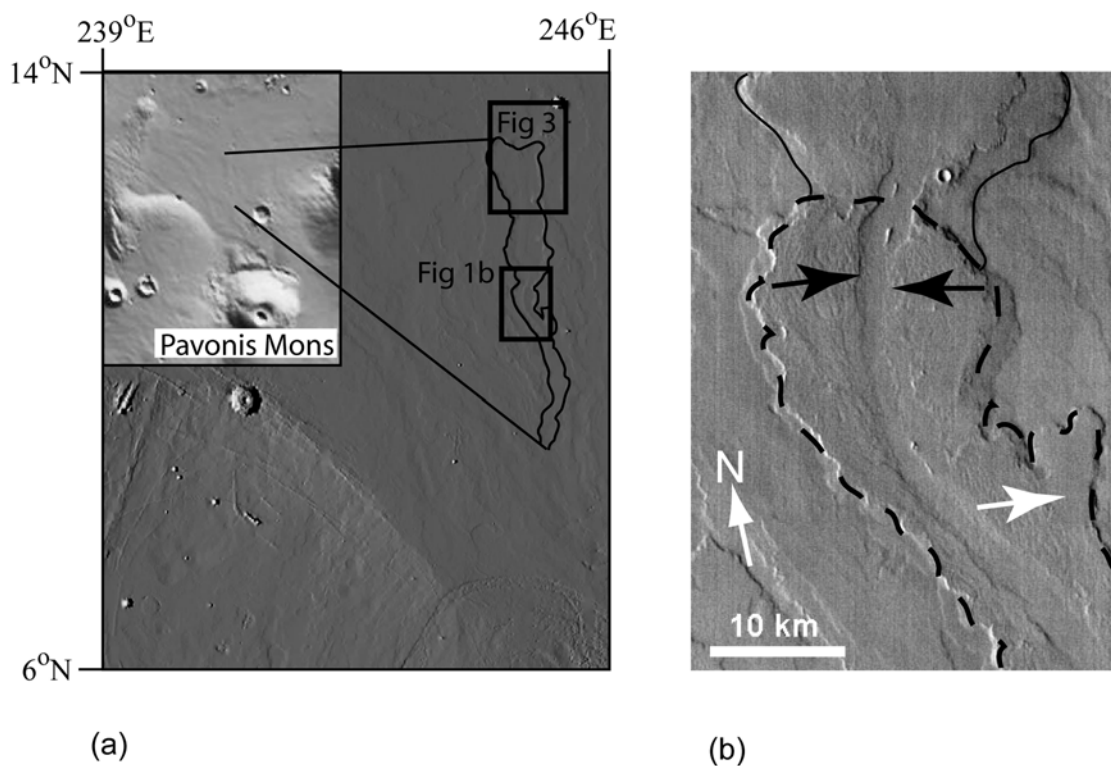


Figure 1. (a) Mars Orbiter Laser Altimeter (MOLA) shaded relief image ($128 \text{ pixels deg}^{-1}$, illuminated from the east) showing the long channelized lava flow north of Pavonis Mons investigated here. The inset shows the location of the lava flow relative to Pavonis Mons, and the boxes indicate the locations of Figures 1b and 3. (b) Thermal Emission Imaging Spectrometer (THEMIS) infrared image (I01739006) of the central channel. Dashed line indicates the flow margin and a possible remnant flow front. Black arrows point to the channel where the flow may have reinitiated, with the subsequent downstream flow margin shown with a solid black line. There is substantial drain down of the channel in this portion of the flow, indicating that lava within the channel was still quite fluid for some time following the emplacement of the collateral levees. The white arrow indicates a possible overspill.

range $10^2 - 10^7 \text{ Pa s}$ [e.g., Walker, 1967; Lipman and Banks, 1987; Moore, 1987; Crisp *et al.*, 1994; Hon *et al.*, 2003]. Inferred viscosities of lava flows on Mars span at least this range, with thicker flows toward the upper end of the viscosity range and vice versa [Zimbelman, 1985; Theilig and Greeley, 1986; Baloga *et al.*, 2003; Leverington, 2004; Greeley *et al.*, 2005; Hiesinger *et al.*, 2007; Garry *et al.*, 2007].

[6] A vertical column within the active component of the lava flow may also have a nondeformable component above the inner fluid core. This upper nondeformable stratum may have a variety of constituents, including solidified lava, partially solidified lava in a nondeformable state, rubble, rafts, etc. For simplicity, the term “crust” will be used in reference to the nondeformable upper component of a vertical column, if it exists, within the active part of the flow.

[7] A great deal of attention has been directed for many years to estimating the rheology of planetary lava flows on the basis of theoretical emplacement models and measured flow dimensions. Previous theoretical models have attempted to obtain rheologic inferences from the dimensions of the channels, levees, the density, and the preexisting slope [e.g., Hulme, 1974; Zimbelman, 1985; Baloga, 1987; Crisp and Baloga, 1990; Baloga *et al.*, 1998, 2003; Rowland *et*

al., 2004; Glaze and Baloga, 2006; Garry *et al.*, 2007]. All these lava flow models are based on some type of simplification of the Navier-Stokes equations and its mathematical solution (e.g., the so-called Jeffreys’ formula). All that can be obtained from flow and levee dimensions using such an approach is a constraint between the active volumetric flow rate and the bulk rheologic properties. Because each of these could vary by many orders of magnitude, modeling the active component alone by a simplification of the Navier-Stokes equations inherently cannot narrow the constraints on emplacement characteristics. Typically, one must input either a range of viscosities or flow rates to develop inferences about emplacement conditions from such fluid dynamic models. Attempts to narrow the range of inferences using thermal dynamics have been largely unsuccessful because most large leveed lava flows on Mars show little or no thickening that would suggest a cooling-induced viscosity change [e.g., Zimbelman, 1985; Mouginitis-Mark and Yoshioka, 1998; Glaze *et al.*, 2003; Baloga *et al.*, 2003; Glaze and Baloga, 2006].

[8] Some models mentioned above assume a central channel already exists within the flow. Others crudely estimate how the levees or stationary margins grow. It is well known from terrestrial experience that the process of levee and stationary margin construction is extremely com-

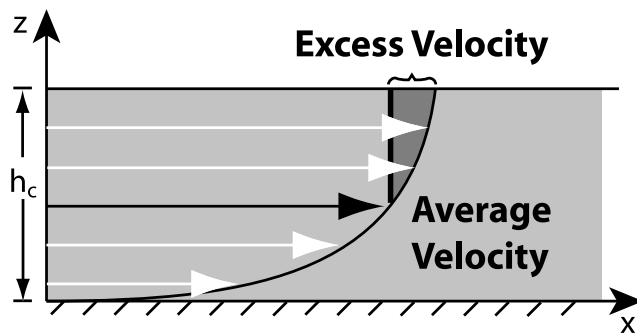


Figure 2. Cartoon illustrating the parabolic velocity profile typical of Newtonian fluids and the concept of “excess velocity” for upper laminae that travel faster than the average. The average velocity, interpreted here as the advance rate of the flow, occurs at a height just below half of the core thickness.

plicated, time-dependent, and subject to a host of random effects [Lipman and Banks, 1987; Moore, 1987; Guest et al., 1987, 1995; Baloga et al., 1998; Hon et al., 2003; Glaze and Baloga, 2006]. From a modeling perspective, the main concern is how the lava volume is conserved, i.e., where and when lava volume transitions from actively participating in the flow advance to a passive role, perhaps confining the active component. Without understanding this lava volume apportioning, the detailed issues of rheology and momentum transfer are academic, at best.

[9] There are a host of morphologic varieties of channelized lava flows on the plains of Mars [Hodges and Moore, 1994; Mougini-Mark and Yoshioka, 1998; Peitersen and Crown, 1999, 2000]. The new model presented here overcomes the fundamental shortcoming of previous theoretical approaches for channelized lava flows that “self-replicate” over long distances. Self-replication means that the morphologic characteristics essentially repeat over the length of the flow, the relative dimensions of the channel and levees are approximately constant, and there is a single channel that can be identified over most of the flow length (Figure 1). Although stagnations, overflows, and time-dependent pulses and lulls in the eruption conditions may have occurred, these processes did not disturb the overall processes of flow advance, levee formation, and central channelization of the flow toward the front. Thus the model does not apply to flows that feature multiple channels or branches or have deposits dominated by stagnations, late stage upstream breakouts, or episodic sources of supply.

[10] To the extent that a channelized lava flow indeed meets the conditions of self-replication, the model provides a significantly improved constraint between viscosity, volumetric flow rate, and emplacement time. The model provides a closed system that constrains these variables without the need to sweep through orders of plausible magnitudes of input parameters. The model considers levees and stationary margins to be formed primarily in a distal zone that is continuously fed by a fully developed, steady state upstream channel. Because of the vertical velocity profile within the upstream flow, the upper portion of the flow core moves faster than the average emplacement

velocity (Figure 2). Thus there exists an excess volumetric flow rate upstream that must be accounted for by shedding of crust, levee construction, a frontal rollover, overflows, breakouts, or surface waves.

[11] In this work, we assume that the excess volumetric flow rate goes into the time-dependent formation of stationary levees in the advancing distal zone. It is well known from terrestrial experience that flows often stagnate, channels become clogged, and upstream overflows and breakouts occur [e.g., Lipman and Banks, 1987; Moore, 1987; Guest et al., 1987, 1995; Hon et al., 2003]. Many of the large channelized flows on Mars seem to have done this as well [e.g., Mougini-Mark and Yoshioka, 1998; Peitersen and Crown, 1999; Garry et al., 2007]. Such possibilities are also considered here, subject to the limitation that the overall self-replicating nature of the channel formation and levee-building processes are not fundamentally disturbed.

[12] With the new model, measured channel and levee dimensions are used to constrain how much crust must have been riding on the deformable core. The inferred thickness of crust is then used with independent thermal arguments to estimate how long it would take to generate crust. This in turn provides bounds on the total emplacement time of the flow, the associated lava viscosity, and the volumetric flow rate. The model is applied to a previously investigated flow north of Pavonis Mons on Mars [Baloga et al., 2003; Glaze and Baloga, 2006]. To assess whether the approach is reasonable, the model is also applied to the 1A flow of the 1984 eruption of Mauna Loa, Hawaii, where there is a great deal of documentation about emplacement conditions, especially the emplacement time [Moore, 1987]. Because the new model depends on an independent estimate of the crustal growth during emplacement, some terrestrial benchmarks are noted to show that the results for the Mars flow are plausible extensions of terrestrial experience. Finally, the sensitivity of the Mars inferences to overflows and upstream breakouts is investigated.

2. Flow Characteristics and Features

[13] The lava flows appropriate for the model presented here have a number of typical characteristics. First, they are long flows that can be traced in excess of a nominal 100 km and feature a prominent central channel. Numerous long channelized flows that extend several hundred kilometers can be found on the Mars plains, although it often becomes difficult to establish unambiguous margins over long distances. Second, the flows appear essentially as a single lobe with a central channel, typically 5–20 km in width. These flows generally have relatively constant channel widths and levee dimensions and show very little thickening with distance. Baloga et al. [2003] suggested that to maintain a near-constant flow thickness (and therefore inferred minimal viscosity increase) for several hundred kilometers, these flows must establish a balance between crust formation and the shedding of material to stationary levees.

[14] The central channels of these flows are visible over great distances on Mars because of substantial drain down. This indicates that some significant fraction of the flow interior was hot and fluid after the construction of the levees. Toward the flow front, it often becomes difficult to identify the drain down because for various reasons (e.g.,

Table 1. Pavonis Mons Lava Flow Dimensions^a

Distance x , km	Slope θ , deg	Flow Width w , km	Channel Width w_c , km	Levee Width w_l , km	Flow Thickness, h_b , m
0	0.07	17.1	6.3	5.4	31
5.5	0.07	17.1	10.8	3.15	36
12.3	0.05	17.1	8.1	4.5	31
19.2	0.05	18.9	9.9	4.5	32
29.7	0.05	18.9	10.8	4.05	47
40.7	0.14	14.4	7.2	3.6	35
49.7	0.14	22.5	12.6	4.95	35
57.1	0.25	19.8	11.7	4.05	46
65.3	0.12	18.9	10.8	4.05	45
74.1	0.06	18	6.3	5.85	48
84	0.1	32.4	13.5	9.45	48
93.4	0.05	25.2	16.2	4.5	49
102.5	0.08	29.7	18	5.85	62
109.7	0.09	24.3	13.5	5.4	53
118.7	0.05	26.1	17.1	4.5	61
126.8	0.03	28.8	14.4	7.2	62
133.1	0.04	27.9	18.9	4.5	60
145.9	0.01	27.9	15.3	6.3	57
154	0.04	36	20.7	7.65	46
160.4	0.05	35.1	23.4	5.85	48
167.6	0.02	39.6	23.4	8.1	50
173	0.05	39.6	27.9	5.85	49

^aAll quantities are measured from Mars Orbiter Laser Altimeter (MOLA) gridded elevation data (128 pixels deg⁻¹).

flat slope or reduced supply) the margin- and levee-building process has stagnated.

[15] Such flows are usually found on the flat plains of Mars, where the regional slope is often very small, usually significantly less than 1° and sometimes only hundredths of a degree. The total widths of these flows, when they can be delineated, and the channel width gently increase with distance [Mouginis-Mark and Yoshioka, 1998; Peitersen and Crown, 1999; Baloga et al., 2003; Garry et al., 2007]. These increases, however, typically amount to only a factor of 2 or 3 at most over the entire length of the flow. Although the overall slopes are small, Mars Orbiter Laser Altimeter (MOLA) data [Smith et al., 1999] indicate that there are slope variations along the flow path. Even though these local variations are very small, (e.g., Table 1), they may cause overflows and breakouts, as well as noticeable changes in flow width and thickness.

[16] The key distinguishing feature of these long channelized flows is the apparent self-replicating nature of the emplacement process. These flows appear to have approximately the same relative dimensions, morphology, and appearance all along the flow path. This is in spite of the gentle widening, thickening, and changes in levee dimensions. There are indications of stagnation, channel clogging, and overflows along the flow path (e.g., Figure 1b). However, these are evidently transient occurrences that are overcome as overall flow advance, channel construction, and distal levee building are resumed. Even at the front of an emplaced flow (e.g., Figure 3), there often remains evidence that the self-replicating emplacement process was still being initiated in the very last stage of flow advance.

[17] The self-replication of the emplacement process suggests a number of points crucial for developing an appropriate model. First, the self-replicating emplacement process is very different from a single-pulse, highly time-dependent process featuring a relatively high initial discharge followed by a long decay in the eruption rate. The

observation that the local morphologic characteristics tend to repeat or change only modestly with distance suggests a protracted, more or less steady state lava supply. This is supported by the continuity of the channel (lack of major breakout lobes), the often-seen drain down, and evidence for the channel construction process at the front. Although it is difficult to sequence the overflows and breakouts from the images presently available, in some sense these must have occurred over timescales and length scales that are small compared to the timescales and length scales of the overall emplacement. Continued feeding of molten lava must have been at a sufficient rate and duration so that stagnations, overflows, and breakouts, to first-order averaged out to a more or less upstream steady state. Otherwise, these effects would have caused total stagnation, failure of the front to advance, and major breakout lobes of the same scale, such as the typical terrestrial analog 1984 Mauna Loa 1, 1A (especially), B, C, and D lobe sequences [e.g., Lipman and Banks, 1987; Moore, 1987]. The subject Mars lava flows do not exhibit any such large-scale breakout lobes.

[18] The flow shown in Figure 1, studied by Baloga et al. [2003] and Glaze and Baloga [2006], is a typical example of a long self-replicating channelized lava flow on Mars. The flow is greater than 200 km in length and was emplaced on slopes much less than 1°. The flow is roughly 50 m thick overall, with an increase of only about 15 m over the final 200 km. Figure 1b is a Thermal Emission Imaging Spectrometer [Christensen et al., 2004] infrared image showing the central channel of the flow. The channel is approximately 15 km across and exhibits substantial drain down. The interpretation here is that the drain down occurred at the end of the eruption, although a variety of other time-dependent scenarios could be envisioned. The flow may have stagnated multiple times, with flow initiating again from each flow front (see example in Figure 1b). The key feature is that no stagnation was significant enough to cause the flow to form a major independent upstream breakout

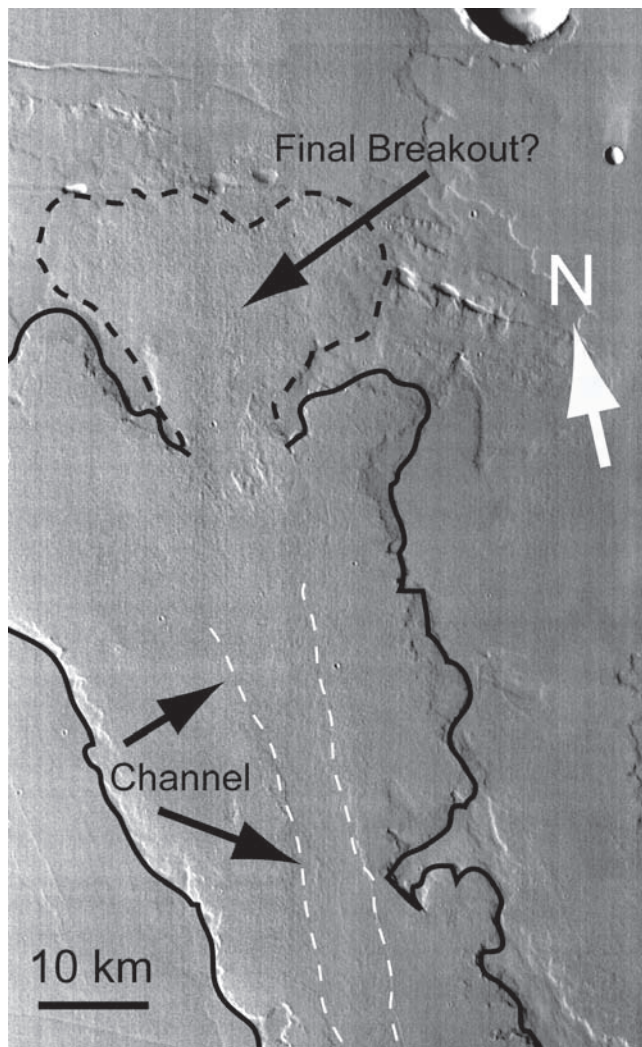


Figure 3. Mosaic of THEMIS infrared images I01739006 and I09391010, showing the distal end of the lava flow in Figure 1. Evidence of a central channel (white dashed lines) exists all the way to the flow front, although the amount of drain down is not as dramatic as seen in Figure 1b. There is also evidence that the self-replication process was attempting to continue through one last small breakout from the final flow front. The probable extent of this final segment of the flow is indicated by the black dashed line.

lobe. Any upstream segment of the flow has essentially the same features and relative dimensions as any other over a distance of more than 200 km. Figure 3 shows the final flow front, where it appears that the self-replicating process was attempting to propagate.

3. Self-Replication Model

3.1. Qualitative Concepts

[19] From a modeling perspective, the main concern is how the lava volume is conserved, i.e., where and when lava volume transitions from actively participating in the flow to an immobile stagnant condition. There are three possible mechanisms for transfer of lava volume from the active to the passive component. With the first mechanism,

lava volume is continuously deposited in the distal zone by the actively advancing front. With the second mechanism, some degree of continuous levee building occurs throughout the length of the flow, while the central channel is forming and even after it is fully developed. Indeed, some success has been achieved using such a spatially dependent model of the levee construction process [Baloga *et al.*, 1998; 2003; Glaze and Baloga, 2006]. The third mechanism involves random and transient overspills and breakouts due to channel clogging, time-dependent pulses and variations in the source conditions, upstream stagnations, levee collapse, and similar processes. The focus here is on the formation of levees in the distal zone (mechanism one), with some attention given to overspills and breakouts (mechanism three). Although levee building may continue along the length of a flow after the channel has been established (mechanism two), Baloga *et al.* [2003] noted that levee widths do not generally decrease with distance along the flow, as one would expect if lava were continuously transferred to the levees. Glaze and Baloga [2006] attempted to address this issue by allowing the lava transfer function to vary as a function of distance. Although the continuous transfer model provided satisfactory results for the Mauna Loa 1984 1A lava flow and a short channelized flow on Mars, the results were less convincing for long self-replicating flows such as the Pavonis Mons flow investigated here. It does not seem likely that the second mechanism is a major contributor to the dynamics of the volume distribution for long self-replicating flows.

[20] The starting point in this work is that the stationary margins are largely emplaced in an advancing distal zone where the construction process is indeed time-dependent (Figure 4). This division is an abstraction of the various zonation documented in field-oriented literature [e.g., Guest *et al.*, 1987; Lipman and Banks, 1987; Hon *et al.*, 2003]. Upstream, the model assumes steady state conditions apply to first-order, except for minor transient events. The sensitivity of the model and our results to significant volumes in the overspills, breakouts, and minor side lobes will be explored in future works.

[21] The self-replicating flow model is constructed by dividing the advancing flow into two zones in the horizontal direction (Figure 5). In the upstream zone, the channel is considered to be fully developed, flowing full, and in steady state. There is no additional growth of the stationary collateral margins. This upstream zone is referred to here as the “channel zone”. Streamlines within the channel zone are assumed to be parallel. Because the channels on Mars are so wide compared to the depth within the channel, circulation near the edges of the channel is ignored.

[22] The “distal zone” is of fixed length and extends from the front of the steady state channel zone to the flow front (Figure 5). Here flow conditions are time-dependent as lava is transferred from the active to the stationary component to construct the embanking levees. As is known from terrestrial experience, lava in this zone consists of a mixture of rubble, cool crust, and varying exposures of hot, fluid interior core. The model presently considers all levee, stationary margin, and channel construction to occur in this distal zone. Streamlines within the distal zone exhibit circulation, time dependence, and randomness. The host of complicated processes as described by Guest *et al.*

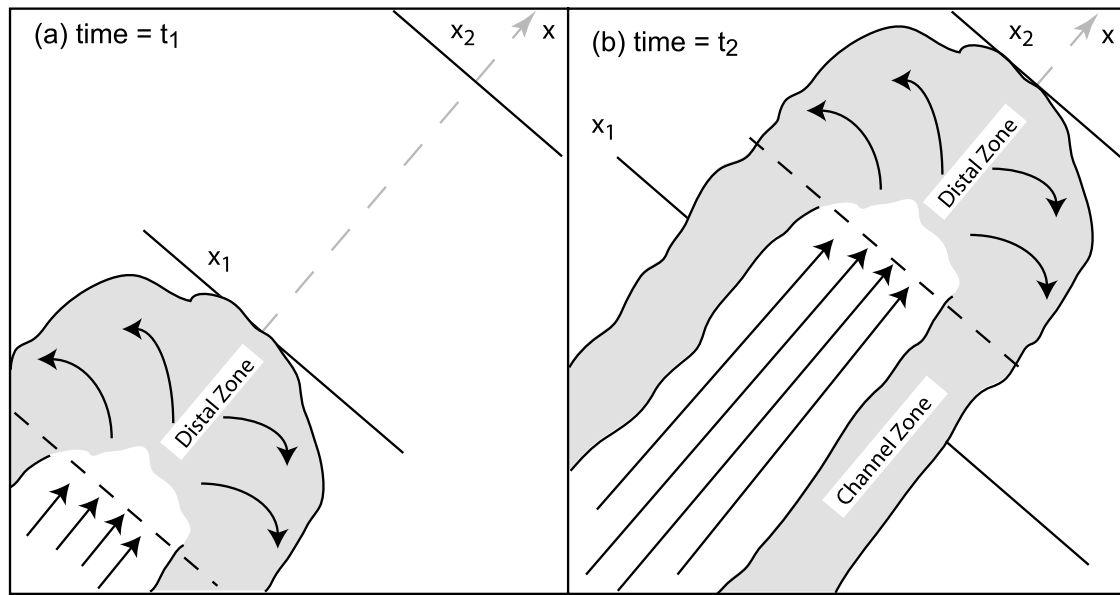


Figure 4. Plan view of an advancing lava flow at times (a) t_1 and (b) t_2 . The lava flow is advancing in the x direction (gray dashed arrow pointing to top right-hand corner). At time t_1 , the lava flow front is located at position x_1 . At time t_2 , the flow front is now located at position x_2 . In both frames, the distal zone of the flow extends from the dark dashed line (cross-flow) to the flow front. In this zone, arrows indicate the transfer of lava from the actively moving lava flow into stationary margins. The channel zone, more visible in Figure 4b, has established levees that are no longer growing.

[1987], *Lipman and Banks* [1987], *Moore* [1987], *Guest et al.* [1995], and *Glaze and Baloga* [2006] that occur near the front make a detailed deterministic treatment impossible. Here we do not worry about the details of levee formation, only that some volume of active lava becomes stationary in the distal zone.

[23] The channel zone is further divided into three vertical zones (Figure 5). The basal part of the molten core consists of all lava from the flow base up to the point where the velocity is equal to the average. Above the basal portion of the core, there is another zone of the core that travels faster than the average but is still deformable. Finally, a solid, nondeformable crust rides on top of the core. The crust affects only the hydrostatic pressure within the flow in the channel zone but none of the other flow properties of the core. The crust travels within the channel zone at the velocity of the upper surface of the core.

[24] There are four key qualitative concepts that form the basis for the new model:

[25] 1. If the flow is self-replicating, flow conditions at the boundary between the channel zone and distal zone must match.

[26] 2. The existence of a hot inner core implies an excess volumetric flow rate in the channel zone. The essence of this concept for a Newtonian vertical velocity profile is illustrated by the cartoon for no crust shown in Figure 2. The critical concept is that there is a height within the molten core above which all fluid laminae travel faster than the average flow velocity. Thus there is a volume of lava in the upper layers that travels faster than the average velocity. This volumetric flow rate is referred to here as the “excess flow rate”. The magnitude of the excess flow rate might not be immediately obvious from Figure 2. The top half of the

flow contains 69% of the total volumetric flow rate or equivalently 2.2 times as much as the lower half (see Appendix A). One can also show that approximately 20% of the total volumetric flow rate is excess, in the sense that the laminae advance with a velocity greater than the average

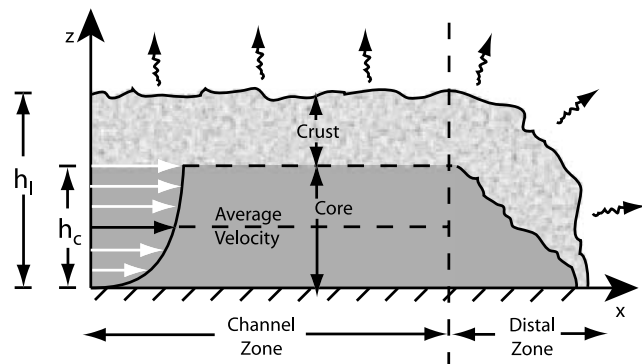


Figure 5. Extension of cartoon in Figure 2, where a solid (nondeformable) crust now rides on top of the molten core. For the self-replication approach, the flow is divided horizontally into channel and distal zones. In the distal zone, complex time-dependent processes transfer material from the advancing flow into stationary margins. In the channel zone, flow within the channel is steady state. For self-replicating flows, conditions at the boundary between the channel zone and distal zone must match. In addition to the nondeformable crust, the deformable core is divided vertically into two zones, above and below the height where lava is moving at the average advance rate. Material above this height is moving with a velocity in excess of the average.

Table 2. Mathematical Notation

Variable	Definition
g	Gravitational acceleration, m s^{-2}
H	Arbitrary height within flow for determining flow rate
h_c	Molten core thickness, m
h_l	Total flow thickness, m
L	Measured flow length, m
L	Length of distal zone, m
L_o	Along flow length of overspill, m
N	Number of overspills of duration Γ_o
Q	Total volumetric flow rate, $\text{m}^3 \text{s}^{-1}$
Q_c	Volumetric flow rate of the core, $\text{m}^3 \text{s}^{-1}$
Q_{ex}	Total excess flow rate, $\text{m}^3 \text{s}^{-1}$
$Q_{\text{ex:c}}$	Excess flow rate in deformable core, $\text{m}^3 \text{s}^{-1}$
$Q_{\text{ex:crust}}$	Excess flow rate in nondeformable crust, $\text{m}^3 \text{s}^{-1}$
Q_o	Volumetric flow rate of overspill, $\text{m}^3 \text{s}^{-1}$
T	Transit time, s
T_o	Transit time when overspills are present, s
Δt	Time for flow front to transit a distal zone length L , s
u_c	Core velocity, m s^{-1}
\bar{u}_c^+	Average excess velocity above z^* , m s^{-1}
\bar{u}_{co}	Reduced average core velocity when overspills are present, m s^{-1}
u_o	Velocity of overspill, m s^{-1}
V_{core}	Core volume, m^3
V_o	Volume of individual overspill, m^3
$V_{\text{overspills}}$	Total overspill volume, m^3
w	Total flow width, m
w_c	Channel width, m
w_l	Levee width, m
x	Horizontal distance coordinate, m
z	Vertical distance coordinate, m
z^*	Height within core where $u_c(z^*) = \bar{u}_c$, m
Γ_o	Time overspill is active, s
μ	Dynamic viscosity, Pa s
ρ	Lava density, kg m^{-3}
θ	Slope, deg

(see Figure 2). This is not of particular theoretical concern for an infinitely long hypothetical flow. However, for an actual, finite, continuously advancing lava flow, this excess flow rate must be accounted for in some fashion.

[27] 3. As a consequence of the second point above, the lava flow advances at the average velocity of the core. Whatever excess volume exists must be continuously converted to levees and margins in the distal zone to maintain the self-replication process.

[28] 4. The crust thickness in the channel zone can be adjusted to explain the volumes that were deposited into the margins and levees. This is significant because independent thermal arguments can subsequently be brought to bear to explain the formation of the crust or the cooling of the excess deformable core. Thus the independent thermal arguments combined with the measured volumes deposited in levees and margins can be used to isolate the emplacement time, the average advance velocity, the viscosity, and the volumetric flow rate.

3.2. Quantitative Concepts

[29] The mathematical notation is given in Table 2. In the channel zone, the lava flow consists of an inner deformable, molten core of thickness h_c . The core may be overlain by a layer of crust or otherwise nondeformable lava so that the total thickness of the flow is h_l . It is assumed that the slope is constant, the channel width is w_c , and the overall flow advances at the average flow velocity of the interior core in the channel zone.

[30] Within the molten core in the channel zone, the vertical velocity profile for a Newtonian fluid is

$$u_c(z) = \frac{\rho g \sin \theta z}{\mu} \left(h_c - \frac{z}{2} \right). \quad (1)$$

From (1), the velocity is zero at the base of the flow, and the upper surface of the core ($z = h_c$) is shear-free, moving with velocity

$$u_c(h_c) = \frac{\rho g \sin \theta h_c^2}{2\mu} = \frac{3}{2} \bar{u}_c, \quad (2)$$

where the average velocity of the core in the channel zone is

$$\bar{u}_c = \frac{\rho g \sin \theta h_c^2}{3\mu}. \quad (3)$$

[31] By (2) and (3), some fraction of the deformable core must travel faster than the average flow velocity. To determine how much flowing lava is excess, the height within the core at which the velocity is equal to the mean velocity must be determined. This height, z^* , is found by equating $u_c(z^*)$, from (1), with the average velocity in (3),

$$\frac{\rho g \sin \theta z^*}{\mu} \left(h_c - \frac{z^*}{2} \right) = \frac{\rho g \sin \theta h_c^2}{3\mu}. \quad (4)$$

Solving (4) for z^* , the interior velocity is equal to the mean value at the height

$$z^* = h_c \left(1 - \sqrt{\frac{1}{3}} \right) = 0.42 h_c. \quad (5)$$

[32] The next step is to determine the excess flow rate within the channel. The average velocity of the deformable core for laminae between z^* and h_c is given by

$$\begin{aligned} \bar{u}_c^+ &= \frac{1}{h_c - z^*} \int_{z^*}^{h_c} u_c(z) dz = \frac{\rho g \sin \theta}{\mu(h_c - z^*)} \left(\frac{h_c^3}{3} - \frac{h_c z^{*2}}{2} + \frac{z^{*3}}{6} \right) \\ &= \frac{4 \rho g \sin \theta h_c^2}{9\mu} = \frac{4}{3} \bar{u}_c. \end{aligned} \quad (6)$$

Thus the excess flow rate of the deformable core laminae above z^* is determined simply by the difference between (6) and (3), multiplied by the cross-sectional area,

$$Q_{\text{ex:c}} = (\bar{u}_c^+ - \bar{u}_c) w_c (h_c - z^*) = \frac{\rho g \sin \theta h_c^3 w_c}{9\sqrt{3}\mu} = \frac{\bar{u}_c w_c h_c}{3\sqrt{3}}. \quad (7)$$

[33] Assuming now that a nondeformable crust layer rides on top of the core, it travels faster than the average velocity as the difference between the velocities in (2) and (3),

$$u_c(h_c) - \bar{u}_c = \frac{\bar{u}_c}{2} = \frac{\rho g \sin \theta h_c^2}{6\mu}. \quad (8)$$

Thus there is also an additional contribution to the excess flow rate from the nondeformable crust of thickness $h_l - h_c$, given by

$$Q_{\text{ex:crust}} = [u_c(h_c) - \bar{u}_c]w_c(h_l - h_c) = \frac{\bar{u}_c w_c (h_l - h_c)}{2}. \quad (9)$$

From the combined deformable and nondeformable layers above z^* , the excess volumetric flow rate that goes into the levee building in the frontal zone is

$$Q_{\text{ex}} = Q_{\text{ex:c}} + Q_{\text{ex:crust}} = \bar{u}_c w_c \left[\frac{h_c}{3\sqrt{3}} + \frac{1}{2}(h_l - h_c) \right]. \quad (10)$$

[34] What remains now is the computation of the levee width constructed in the distal zone from the excess flow rate in (10). Levees are assumed to be symmetrical and roughly triangular in cross section with heights the same as the total flow thickness, h_l , and widths denoted by w_l . Let Δt be the time required for the flow front to transit a distal zone length L , and thus $\Delta t = L\bar{u}_c$. During this time interval, the excess volume of $Q_{\text{ex}}\Delta t$ constructs a levee of volume $1/2 w_l h_l L$ on each side of the flow. Thus $Q_{\text{ex}}L\bar{u}_c = w_l h_l L$, and by (10), the levee width is given by

$$w_l = \frac{Q_{\text{ex}}}{\bar{u}_c h_l} = \frac{w_c}{h_l} \left[\frac{h_c}{3\sqrt{3}} + \frac{1}{2}(h_l - h_c) \right]. \quad (11)$$

[35] Once the dimensions of the channel and levees are known, (11) can be solved for molten core thickness (see the example in section 4).

[36] It is somewhat remarkable that so many factors cancel out in this formulation of the levee construction process. Plausible values of the emplacement time, Reynolds's number, flow velocity, and viscosity might change by many orders of magnitude. However, according to the self-replicating model, i.e., (11), most of their mutual interactions offset with regard to the levee dimensions. This in part is why large leveed lava flows appear so similar in different volcanic provinces on Mars and, indeed, on different planetary surfaces.

4. Applications of the Self-Replication Model

[37] A long flow north of Pavonis Mons has been chosen as an application because its dimensions have been docu-

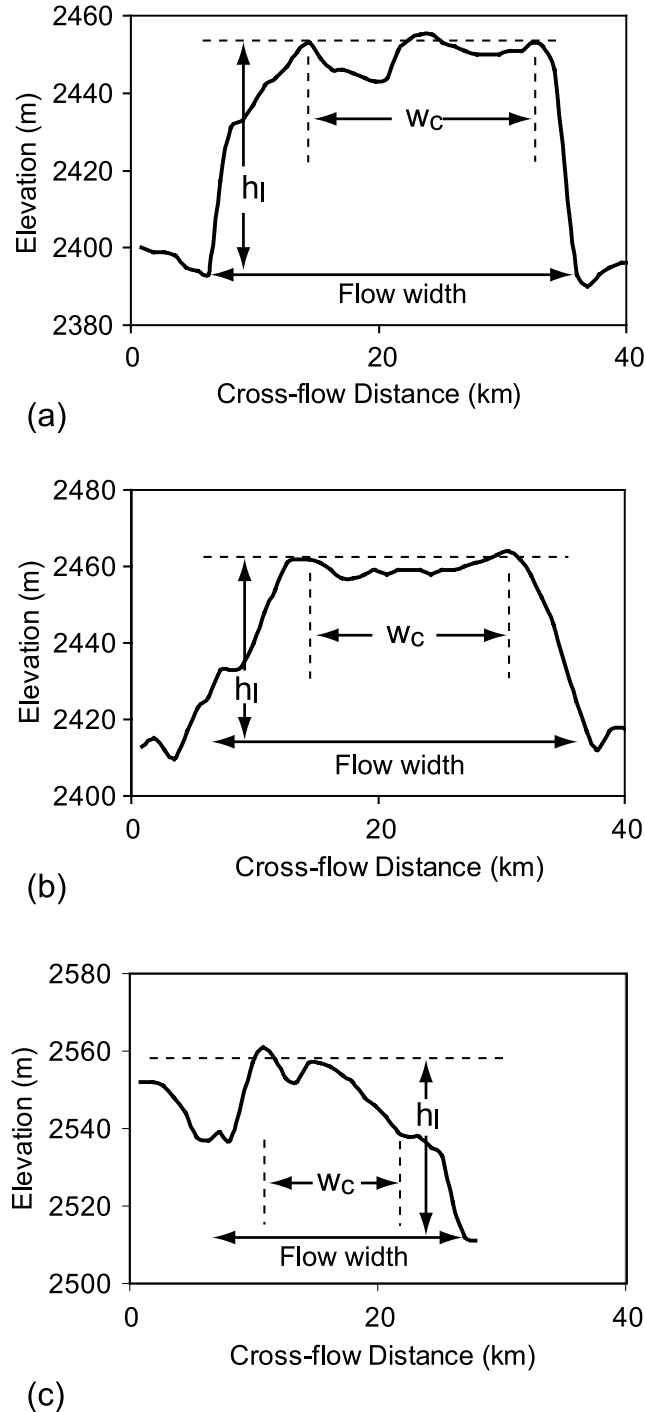


Figure 6. Three cross-flow profiles from MOLA gridded data for the Pavonis Mons flow illustrating how the flow thickness (h_l), channel width (w_c), and total flow widths are determined. Profiles are (a) 10, (b) 11, and (c) 18, from Baloga *et al.* [2003]. Locations of all profiles used here are shown by Baloga *et al.* [2003]. The levee widths reported in Table 1 are equal to half of the difference between total flow width and channel width. In each case, the extent of the channel is taken to be the high point of the levee. However, individual profiles each require careful examination to interpret the flow dimensions. For example, Figure 6a seems to indicate that two channel-forming events may have occurred at that location. Our interpretation is that the outer levee was emplaced as the flow front passed and the inner levee formed at a later time. Thus outer levee dimensions were used in the model calculations. Figure 6b is relatively straightforward, as the channel is clearly visible. However, determination of the outer margin of the flow requires comparisons to image data. Figure 6c has a cross-flow slope. The change in elevation across the flow makes it difficult to interpret the channel width precisely. This is not uncommon. However, such imprecision has little effect when the channel width is much greater than the flow thickness.

mented previously in the literature [Baloga *et al.*, 2003; Glaze and Baloga, 2006]. The flow can be traced definitively back from the flow front for almost 200 km. Although the flow appears to possibly originate another 100 km upstream, toward the saddle between Pavonis and Ascræus Montes, it becomes quite difficult to unambiguously identify the flow margins. Because of this ambiguity, only those cross-flow profiles collected by Baloga *et al.* [2003] over the final 173 km have been used here. Table 1 shows the basic dimensional parameters for the Pavonis Mons lava flow shown in Figures 1 and 3. The individual point-to-point slopes reported in Table 1 were derived from a transect along the flow centerline in the gridded MOLA data. The reported values are simply the slopes between elevations at each cross-flow profile. Although one can argue that the underlying slope is not precisely reflected in the flow surface, the minimal flow thickening and long distances imply that these slopes are reasonable estimates.

[38] The data used here were derived from the same 22 cross-flow profiles discussed by Baloga *et al.* [2003]. However, the channel and levee widths used here differ slightly from those reported in that paper. The prior work was not sensitive to differences of a few percent in the ratio of levee volume to total flow volume. The model presented here, however, requires more precision regarding how the channel margins are chosen. Thus all 22 cross-flow profiles have been reassessed in a consistent manner appropriate to this study. Three such example profiles are shown in Figure 6. The locations of the channel and flow margins are also indicated. In general, the “high water mark”, i.e., highest point on each levee, was chosen as the outer extent of the channel.

[39] The information in Table 1 is all that is required to estimate the crust thickness for this flow. For each step, the local values for slope, channel width, and channel thickness are used to estimate the amount of crust required to generate levees of width w_l on each side. Equation (11) is used at each location along the flow by stepping through a range of values for the core thickness, h_c , until the resulting w_l matches the measured levee widths indicated in Table 1. In general, levees for the Pavonis flow appear to be well described by a triangular shape, as required by (11). Some of the cross-flow profiles do show levees that might be better described by a rectangle, but these do not appear to be the norm. The resulting core depths and crust thicknesses for each of the 22 locations along the flow are given in Table 3.

[40] Most of the crust thickness estimates in Table 3 seem plausible, ranging between 1 and 20 m. However, there is a great deal of variability present in the results, making it difficult to identify any significant trends. This is a very common problem when dealing with real natural data. The variations are so prominent that it is sometimes difficult to discern the underlying systematic tendencies. Figure 8 includes the computed crust thicknesses as a function of distance and is typical of lava flow dimension charts. It is completely clear that a direct regression analysis would have no statistical validity because of the degree of variability in the data. Moreover, some degree of negative correlation is anticipated between changes in the thickness of the crust and changes in channel width, i.e., as

Table 3. Flow Dimensions^a

Distance x , km	Channel Width w_c , km	Flow Thickness h_l , m	Core Thickness h_c , m	Crust Thickness $h_l - h_c$, m
0	6.3	31	15	16
5.5	10.8	36	33	3
12.3	8.1	31	22	9
19.2	9.9	32	26	6
29.7	10.8	47	40	7
40.7	7.2	35	27	8
49.7	12.6	35	30	5
57.1	11.7	46	41	5
65.3	10.8	45	39	6
74.1	6.3	48	21	27
84	13.5	48	29	19
93.4	16.2	49	46	3
102.5	18	62	56	6
109.7	13.5	53	45	8
118.7	17.1	61	58	3
126.8	14.4	62	47	15
133.1	18.9	60	58	2
145.9	15.3	57	47	10
154	20.7	46	40	6
160.4	23.4	48	46	2
167.6	23.4	50	44	6
173	27.9	49	48	1

^aWidths and thicknesses are estimated from MOLA gridded elevation data (128 pixels deg⁻¹). Individual core and crust thicknesses are obtained by adjusting ratio to match the local levee volume.

a channel widens, a thinning of what we have called crust is anticipated.

[41] Both of these effects are addressed by an alternative approach to a direct regression analysis of the crust thickness. First, the level of noise can be reduced substantially by dealing with accumulated data [e.g., Glaze and Baloga, 2006]. Second, the cumulative tendency in crust thickness will be normalized by the cumulative tendency in channel width. Figures 7a and 7b show plots of accumulated values for $w_c(h_l - h_c)$ (the cross-sectional area of the crust at each position along the flow) and w_c . These cumulative curves can be described by the regressions (where w_c and x are in km, and h_l and h_c are in m)

$$w_c(h_l - h_c) = 0.0216x^2 + 8.203x + 69.97 \quad (12)$$

$$w_c = 0.0058x^2 + 0.6372x + 16.25 \quad (13)$$

respectively.

[42] Both of these regressions are very good fits to the accumulated data (R^2 values of 0.994 and 0.996, respectively). Dividing the regression in (12) by (13) at each location, x , gives a “smoothed” estimate of the crust thickness along the flow and clarifies the trend in crust formation along the flow (Figure 8). Note that the initial crust thickness is not zero at $x = 0$ because the starting point is simply the farthest point upstream where the flow can be unambiguously identified and measured. This starting point for the analysis ($x = 0$) appears to be at least 100 km from the probable vent location. The crust shows a slight amount of thinning toward the flow front as a result of the gentle widening of the flow.

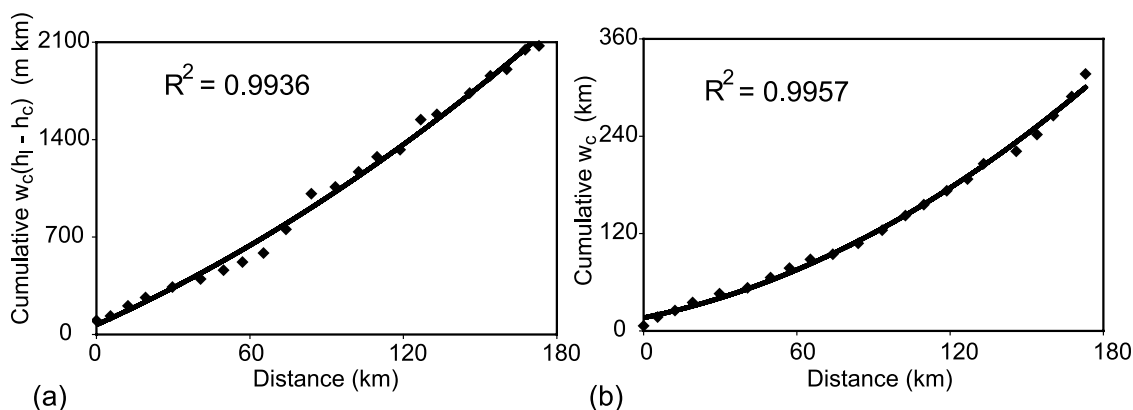


Figure 7. Plots of (a) cumulative $w_c(h_l - h_c)$ and (b) cumulative w_c for the Pavonis Mons lava flow. The data are shown as black diamonds, and the least squares regression for each curve is shown with a solid black line. Both sets of cumulative data are well fit by a second-order polynomial regression. Parameters for the fits are given in (12) and (13).

[43] The crust thickness estimated for the Pavonis Mons lava flow is consistent with those measured for basaltic lava flows with a broad range of sizes on Earth. Figure 9 compares, conceptually, the Pavonis Mons lava flow to cross-sectional profiles for large-scale (Columbia River Basalt Group (CRBG)) and small-scale (Kilauea, Hawaii) terrestrial flows, as observed by *Thordarson and Self* [1998] and *Thordarson* [2000]. In an absolute sense, the 8 m crust estimated for the Pavonis Mons flow is very similar to the 8 m crust observed for the Levering flow within the CRBG. On a relative basis, the proportional thickness to total flow thickness is somewhat less for the large Mars flow.

[44] The emplacement duration for the last 173 km can now be inferred from the thermal dynamics of crust growth. Figure 10 shows the time required to solidify the upper surface of lava flowing in the channel to a depth of ~ 8 m, assuming the conductive cooling law used by *Hon et al.* [1994, and references therein]. These calculations cool the lava from 1142°C to 1070°C at the depth indicated by the theoretical curve. The intersection of the inferred crustal thickness and the theoretical crustal growth curve indicates the emplacement time on the horizontal axis of Figure 10. Thus approximately 600 d are required to attain the 8 m of crust shown in Figure 8. The preferred emplacement time for the Pavonis flow is approximately 2 years and perhaps 3 years when the full 300 km extent of the flow is considered.

[45] Because this flow is so thick and wide (compared to its thickness), the conductive model is probably appropriate for estimating the emplacement time. If it were thinner, variations in the ambient topography could be a significant influence on disrupting the crust [e.g., *Crisp and Baloga*, 1990; *Glaze and Baloga*, 2007], thus converting more core into crust. Similarly, for a flow that is narrower, exposure of the circulating molten interior at the shear margins could become relatively more significant. Surface cracks, shear margins, and other processes that lead to molten core exposure diminish the time required to form the required amount of crust. Terrestrial experience suggests the emplacement time could be reduced by a factor of 2 because of these influences.

[46] For comparison, the self-replication approach has also been applied to the well-documented 1984 1A lava flow at Mauna Loa. Figure 11 shows curves for crust thickness assuming only conductive cooling, as well as an extreme case of 10% [*Crisp and Baloga*, 1990; *Crisp et al.*, 1994] exposed core that cools radiatively. For this flow, the emplacement time is a known quantity, approximately 7 d [*Moore*, 1987]. Using the flow dimensions in work by *Glaze and Baloga* [2006], the maximum crust thickness for this flow is ~ 3.5 m, as calculated by the self-replication model. This estimate is consistent with modest radiative cooling from cracks and is in very good agreement with the estimate by *Crisp et al.* [1994].

[47] Once the emplacement time is known, the dynamic viscosity of the molten core can be determined. The subsequent computations use 3.73 m s^{-2} and 2600 kg m^{-3} for the Mars gravity and lava density, respectively. The previously computed local core thicknesses and local slopes provide the average core velocities and transit times for each distance increment along the flow path for any given viscosity by (3).

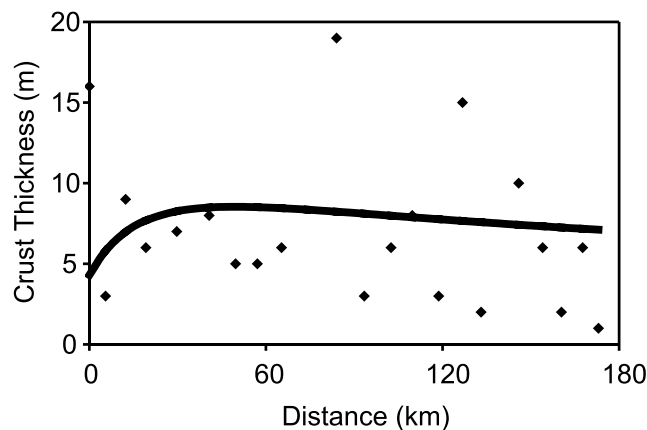


Figure 8. Crust thickness estimates for the Pavonis Mons flow. Diamonds indicate individual estimates from Table 3. Smooth curve is determined from the regressions on the cumulative values in Figure 7 (see text for discussion).

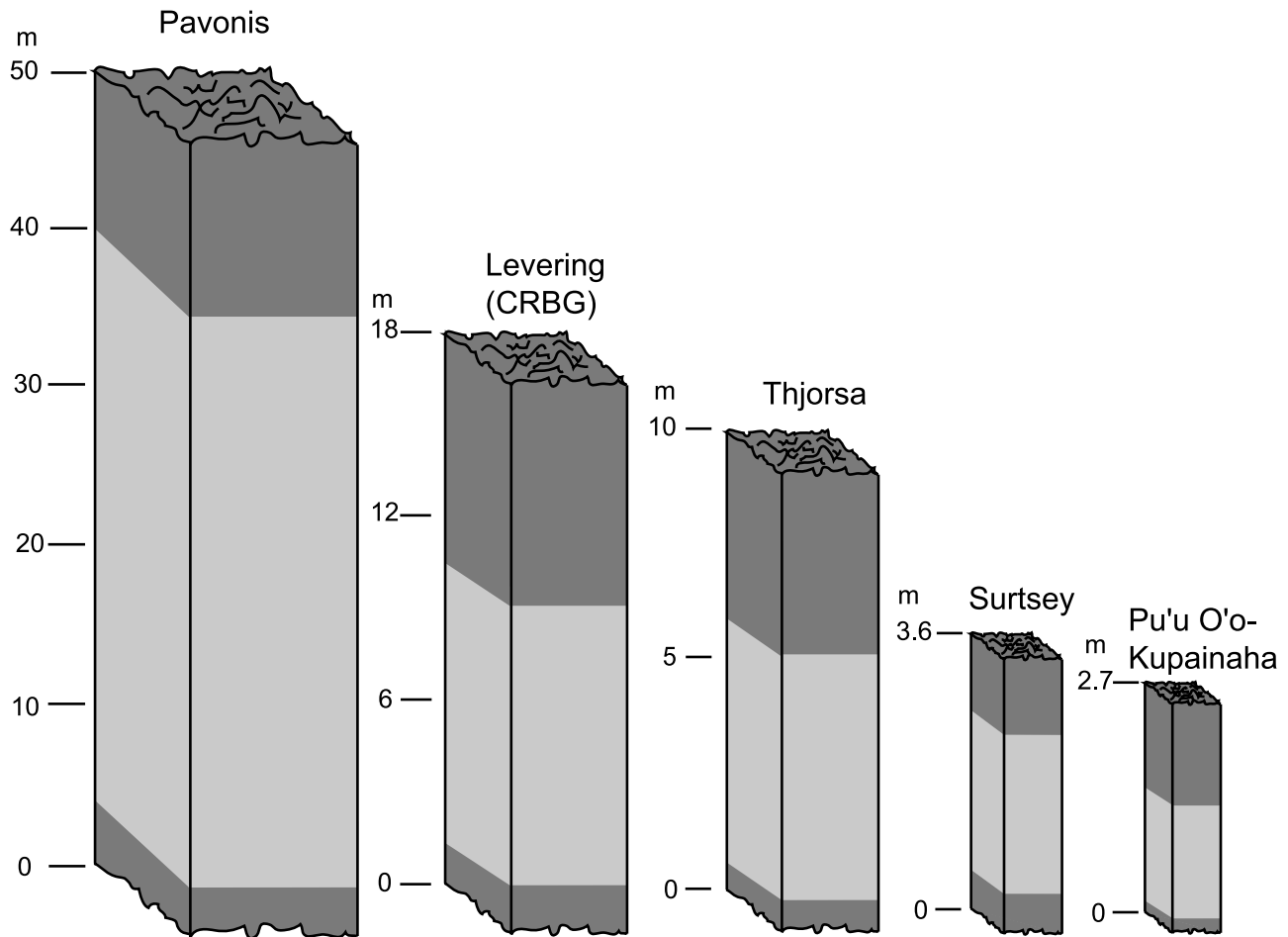


Figure 9. Comparison of a theoretical columnar core/crust profile through the Pavonis Mons lava flow and several terrestrial analogs. Light and dark gray regions correspond to flow core and crust, respectively. The figures for the Levering flow (part of the Columbia River Basalt Group, Washington), Thjorsa flow (Iceland), and Pu'u O'o Kupainaha (Hawaii) are based on Figure 20 in work by *Thordarson and Self* [1998]. The Surtsey (Iceland) data are based on Figure 7 by *Thordarson* [2000]. The vertical scales for each flow are indicated.

When the molten core viscosity is 1.36×10^6 Pa s, the sum of the incremental transit times over 173 km is 600 d. An increased heat loss rate of a factor of 2 would diminish both the emplacement time and the estimate of the viscosity by the same factor.

[48] The emplacement time also implies an estimate of the flow rate for the Pavonis Mons flow. The average flow velocity is about 0.0033 m s^{-1} ($173 \text{ km } 600 \text{ d}^{-1}$). Using the average channel width of 14.4 km and the average flow thickness of 46.86 m, the corresponding volumetric flow rate is about $2250 \text{ m}^3 \text{ s}^{-1}$. Such a flow rate compares favorably with terrestrial experience, considering the overall cross-sectional area of the Pavonis flow. For the main flows from 1984 Mauna Loa eruption, field-based estimates of the volumetric flow rate range from about 300 to $500 \text{ m}^3 \text{ s}^{-1}$ [*Lipman and Banks, 1987; Moore, 1987; Rowland and Walker, 1990*]. In contrast to the Pavonis flow, the 1984 Mauna Loa flow complex is an order of magnitude smaller in length, issued from centralized vents and is at least 3 times thinner in thickness. Other terrestrial eruptions have been thought to produce eruption rates on the order of

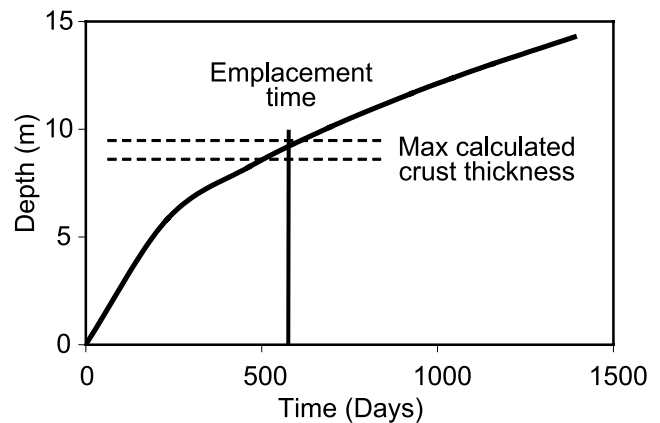


Figure 10. Thickness of crust, generated solely by conductive cooling as a function of time (in d), is shown as the solid black curve. The horizontal dashed lines indicate a range of estimated crust thickness for the Pavonis Mons lava flow (Figure 8). The cooling curve and the estimated crust thickness lines intersect at roughly 600 d, interpreted as the time of emplacement for the final 173 km of the flow.

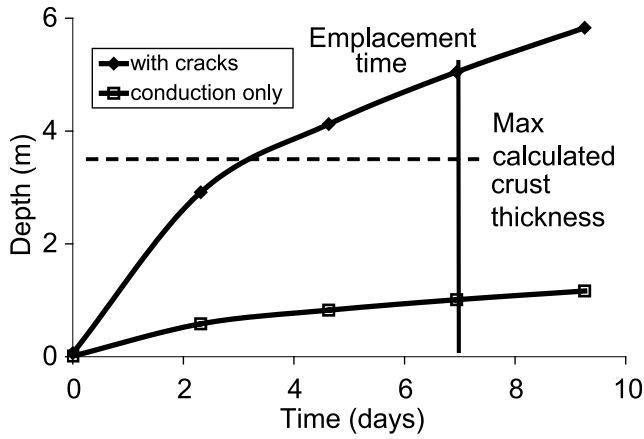


Figure 11. The two solid black curves indicate the thickness of crust for both the conductive cooling–only case, as well as a case for combined conductive and radiative cooling with 10% cracks (by area). Significant cracks were observed in the surface crust for the Mauna Loa 1984 1A lava flow during emplacement. The horizontal dashed line indicates the ~ 3.5 m crust thickness for the Mauna Loa 1984 1A flow as estimated by the model. The emplacement time of 7 d (vertical solid line) is well known for this flow and indicates that ~ 3.5 m of crust is consistent with a combination of conductive cooling and a small degree of radiative cooling.

$1000 \text{ m}^3 \text{ s}^{-1}$, for example, Mauna Loa in 1950, Hualalai in 1801, and the Great Crack eruption of Kilauea in 1823 [Malin, 1980; Rowland and Walker, 1990; Baloga et al., 1995, and references therein]. The key difference indicated by this analysis, however, is that the terrestrial eruptions were not sustained for the long duration inferred for the Pavonis Mons flow.

5. Influence of Overspills

[49] Stationary margins of long channelized lava flows do not always form solely in the frontal zone. Another significant mechanism for forming stationary margins is through overspills and breakouts [e.g., Guest et al., 1987, 1995; Lipman and Banks, 1987; Moore, 1987; Baloga et al., 2003; Hon et al., 2003; Rowland et al., 2004; Glaze and Baloga, 2006; Woodcock and Harris, 2006; Garry et al., 2007]. These occur upstream in the channel zone when the flow stagnates, the channel becomes clogged, a levee collapses, or there is a surge in the supply rate. To avoid repetition, the term “overspill” will be used subsequently in reference to overspills, upstream breakouts, minor side lobe formation, and other features constructed by transient upstream processes.

[50] Overspills influence the estimates of emplacement time, viscosity, and flow rate obtained in section 4. Overspills have the following effects: (1) By bleeding off lava from the channel, less flow rate is delivered to the distal zone. (2) The flow rate within the core is reduced, so the average velocity of advance diminishes. (3) The diminished advance rate implies a greater time for the front to advance a

given distance. (4) There is more time for the core to form more crust.

[51] To estimate the influence of overspills, the following assumptions are made. First, they occur only in the channel zone and are small enough for the self-replication process to continue in the distal zone. Second, only volume removals from the core are considered. Such removals would have the greatest influence on the advance rate and the formation of crust.

[52] For simplicity, an overspill is considered to occur over some fixed upstream length, L_o , and to persist for a fixed time Γ_o . The subscript o in this section indicates that overspills are present. All other variables have the same meaning as before. Volume is removed from the core by an effective flow rate given by

$$Q_o = u_o h_c L_o. \quad (14)$$

[53] It is assumed that throughout the duration of emplacement, such a breakout occurs somewhere upstream of the distal zone. Each overspill transfers a total volume $V_o = Q_o \Gamma_o$ from the active part of the flow to the stationary components. In the limiting case, once an overspill has ended, a new one begins somewhere else upstream.

[54] The reduced average velocity of the core when overspills are present is represented by the subscript co . When overspills are present, the volumetric flow rate in the core will be diminished according to

$$Q_c = h_c w_c \bar{u}_{co} = h_c w_c \bar{u}_c - \frac{V_o}{\Gamma_o}. \quad (15)$$

Thus the front advances at the diminished rate

$$\bar{u}_{co} = \bar{u}_c - \frac{V_o}{h_c w \Gamma_o}. \quad (16)$$

[55] Equation (16) gives the change in the transit time due to the existence of the overspills. Denoting T and T_o as the flow front transit times to a distance L when no overspills and overspills are present, respectively,

$$L = \bar{u}_c T = \bar{u}_{co} T_o \quad (17)$$

So from (16) and (17),

$$T_o = T \left(1 - \frac{TV_o}{\Gamma_o h_c w_c L} \right)^{-1} \quad (18)$$

[56] As a bounding case, a single overspill continuously exists at all times, so that $T = N\Gamma_o$. Thus the total overspill volume is given by $V_{\text{overspills}} = NV_o$. When this is used in (18), the transit time when overspills are present is given by

$$T_o = T \left(1 - \frac{NV_o}{h_c w_c L} \right)^{-1} = T \left(1 - \frac{V_{\text{overspills}}}{V_{\text{core}}} \right)^{-1}. \quad (19)$$

[57] Equation (19) shows how to calculate the increase in the duration of emplacement due to overflows. It requires an estimate of the total volume of overflows, $V_{\text{overflows}}$, relative to the total core volume within the channel, V_{core} . As noted in prior works [Baloga *et al.*, 1998, 2003; Glaze and Baloga, 2006], there is obviously a limit to the amount of lava that can be bled off from the active component before the flow front ceases to advance. Further, for self-replication to be valid, overflows must be a relatively minor process. The range between about 10 and 50% for the volume ratio in (19) implies emplacement times 1.1–2 times longer than those estimated with no overflows.

6. Conclusions

[58] A new model for long self-replicating channelized lava flows on the Mars plains has been developed. This new model provides constraints on emplacement conditions (e.g., viscosity and volumetric flow rate) that are not obtainable by previous formulations that assume levees are formed along the entire length of the lava flow throughout the duration of emplacement [Baloga *et al.*, 1998, 2003; Glaze and Baloga, 1998, 2006]. Even by exploring constant and spatially variable rates of lava transfer to the levees, none of the prior models adequately addresses time-dependent distal stationary margin formation. The new approach more closely resembles terrestrial field observations, particularly when the influence of upstream overflows and breakouts is included.

[59] The key feature of long channelized lava flows on Mars is self-replication of the emplacement process over distances often exceeding 100 km. Any stagnations, overflows, channel clogs, or breakouts evident in Mars images must have been transient events because the flows self-replicate their morphologies and relative dimensions over such great distances. The self-replication approach uses measured levee and channel dimensions to estimate the relative crust and core thicknesses. The subsequent use of plausible thermal models for crustal growth in turn provides a true constraint on the duration of emplacement and the viscosity of the molten core. Once these quantities are known, related quantities such as volumetric flow rate and advance velocity can be inferred directly.

[60] The new model assumes levees form primarily in an advancing distal zone, while the upstream channel zone is in steady state. Once the flow front has passed, levee formation ceases. To self-replicate, conditions within the channel and distal zones must match at the interface. When the hot inner core of the channel zone has a velocity profile, there is lava near the surface that moves faster than the average velocity. The excess flow rate associated with this material forms the levees in the distal zone. The thickness of crust riding on top of the hot inner core can be adjusted to accommodate differences between the levee volumes estimated from the excess volumetric flow rate and observed levee volumes.

[61] The self-replication model was applied to an exemplary channelized lava flow north of Pavonis Mons that is >200 km in length. Channel and levee dimensions for this flow are roughly constant along the length of the flow, with some modest thickening and widening. Results indicate that a significant crust, ~ 8 m thick, must have formed during

emplacement in order to maintain the balance between levee volume and the excess flow rate in the upstream channel. This crustal thickness is consistent with observations of terrestrial lava flows in Hawaii, Iceland, and the Columbia River Basalt Group. The time required to grow such a crust through conductive cooling is about 600 d, interpreted here as the emplacement time. This emplacement time, in turn, implies a core viscosity on the order of 10^6 Pa s, an advance rate of 0.0033 m s^{-1} , and a flow rate of 2250 m³ s^{-1} . With the exception of emplacement time, these values represent only modest extrapolations of terrestrial experience.

[62] The model has also been applied to the Mauna Loa 1984 1A lava flow, where the emplacement time and other dimensional parameters have been well documented. The results show that the formalism for crust formation and shedding is indeed a reasonable approach. The new model predicts a distal crust thickness of ~ 3.5 m on the basis of the levee and channel dimensions. Constrained by the known 7 d emplacement time, this crust thickness is consistent with modest combinations of conductive and radiative cooling (less than 10% of exposed core).

[63] The most important implication of the self-replication model is that the long channelized lava flows on the plains of Mars are only modest extrapolations of terrestrial experience. The primary difference is that high eruption rates must have persisted on Mars for durations on the order of years, rather than hours or days as is typical for terrestrial flows. The persistent lava supply, in turn, provides the Martian flows with the opportunity to establish an approximate balance between the formation of crust and the transfer of lava to stationary components. Although the same processes operate in smaller terrestrial analogs, such a balance is difficult to establish because of the shorter eruption durations for terrestrial flows. Moreover, lower terrestrial flow rates mean that flows are thinner and thus more susceptible to transient events (e.g., surges, blockages, and overflows) and the influence of small-scale topography.

[64] The inclusion of overflows in the example Mars flow application shows that the emplacement time would increase only by a factor of about 2. Emplacement durations longer than 1200 d would require more of the levee volume to be formed by overflows and would have significantly disrupted the self-replicating nature of the flow. Future work on the self-replication formalism will address the effects of transient overflows and upstream breakouts through detailed simulations where the locations, durations, and volumes of overflows are varied randomly.

[65] Large (>100 km) self-replicating channelized lava flows appear to be common on the Mars plains. However, exact flow margins are frequently ambiguous, as lobes and segments of many flows often coalesce. Thus it may be that isolated long channelized flows, such as the one examined here, represent a penultimate evolutionary stage. Longer eruption times at comparable high flow rates may produce flows completely dominated by stagnations, overflows, and breakouts. Such conditions probably lead to the often-seen indistinguishable amorphous mass of lobes and segments, where no single flow can be delineated for more than a few tens of kilometers. Further understanding of emplacement conditions would advance our interpretation of plains vol-

canism on Mars with implications for the character and persistence of sources of subsurface magma supply.

Appendix A

[66] The velocity profile in (1) is used to compute the flow rate for any height H within the flow. For simplicity, it is assumed that there is no overriding crust. By definition, the volumetric flow rate from the base to a height H is given by

$$Q_H = w_c H \bar{u}_c(0 < z < H) = w_c H \left(\frac{1}{H} \int_0^H u_c(z) dz \right). \quad (\text{A1})$$

When there is no crust and $H = h_l$,

$$Q = Q_{hl} = \frac{\rho g \sin \theta h_l^3 w_c}{3\mu} \quad (\text{A2})$$

is the familiar total flow rate for a Newtonian fluid. In the lower half of the flow up to $H = h_l / 2$ the flow rate is

$$Q_{h_l/2} = \frac{5}{16} Q. \quad (\text{A3})$$

Thus the upper half of the flow contains the flow rate

$$Q_{z \geq h_l/2} = \frac{11}{16} Q = 0.6875 Q. \quad (\text{A4})$$

To state this another way, 2.2 times more flow rate is contained in the upper half of the flow than the lower half.

[67] **Acknowledgments.** This work was supported by the NASA Mars Data Analysis Program, grants NNX06AD98G and NNG04GN05G. The authors appreciate the detailed and thoughtful reviews by David Crown and Scott Rowland. SMB would also like to thank Stephen Mackwell and scientists at the USRA Lunar and Planetary Institute, Houston, Texas for their encouragement and support during part of this research.

References

- Baloga, S. (1987), Lava flows as kinematic waves, *J. Geophys. Res.*, *92*(B9), 9271–9279.
- Baloga, S., and D. C. Pieri (1986), Time-dependent profiles of lava flows, *J. Geophys. Res.*, *91*(B9), 9543–9552.
- Baloga, S. M., P. D. Spudis, and J. E. Guest (1995), The dynamics of rapidly emplaced terrestrial lava flows and implications for planetary volcanism, *J. Geophys. Res.*, *100*(B12), 24,509–24,519.
- Baloga, S. M., L. S. Glaze, J. A. Crisp, and S. A. Stockman (1998), New statistics for estimating the bulk rheology of active lava flows: Puu Oo examples, *J. Geophys. Res.*, *103*(B3), 5133–5142.
- Baloga, S. M., P. J. Mougini-Mark, and L. S. Glaze (2003), Rheology of a long lava flow at Pavonis Mons, Mars, *J. Geophys. Res.*, *108*(E7), 5066, doi:10.1029/2002JE001981.
- Christensen, P. R., et al. (2004), The Thermal Emission Imaging System (THEMIS) for the Mars 2001 Odyssey mission, *Space Sci. Rev.*, *110*, 85–130.
- Crisp, J. A., and S. M. Baloga (1990), A model for lava flows with two thermal components, *J. Geophys. Res.*, *95*(B2), 1255–1270.
- Crisp, J. A., K. V. Cashman, J. A. Bonini, S. B. Houghton, and D. C. Pieri (1994), Crystallization history of the 1984 Mauna Loa lava flow, *J. Geophys. Res.*, *99*(B4), 7177–7198.
- Daneš, Z. F. (1972), Dynamics of lava flows, *J. Geophys. Res.*, *77*(8), 1430–1432.
- Garry, W. B., J. R. Zimbelman, and T. K. P. Gregg (2007), Morphology and emplacement of a long channelized lava flow near Ascraeus Mons Volcano, Mars, *J. Geophys. Res.*, *112*, E08007, doi:10.1029/2006JE002803.
- Glaze, L. S., and S. Baloga (1998), Dimensions of Pu'u O'o lava flows on Mars, *J. Geophys. Res.*, *103*(E6), 13,659–13,666.
- Glaze, L. S., and S. M. Baloga (2006), Rheologic inferences from the levees of lava flows on Mars, *J. Geophys. Res.*, *111*, E09006, doi:10.1029/2005JE002585.
- Glaze, L. S., and S. M. Baloga (2007), Topographic variability on Mars: Implications for lava flow modeling, *J. Geophys. Res.*, *112*, E08006, doi:10.1029/2006JE002879.
- Glaze, L. S., S. Baloga, and E. R. Stofan (2003), A methodology for constraining lava flow rheologies with MOLA, *Icarus*, *165*, 26–33.
- Greeley, R., and D. A. Crown (1990), Volcanic geology of Tyrrhena Patera, Mars, *J. Geophys. Res.*, *95*(B5), 7133–7149.
- Greeley, R., B. H. Foing, H. Y. McSween Jr., G. Neukum, P. Pinet, M. vanKan, S. C. Werner, D. A. Williams, and T. E. Zegers (2005), Fluid lava flows in Gusev crater, Mars, *J. Geophys. Res.*, *110*, E05008, doi:10.1029/2005JE002401.
- Guest, J. E., C. R. J. Kilburn, H. Pinkerton, and A. M. Duncan (1987), The evolution of lava flow-fields: Observations of the 1981 and 1983 eruptions of Mount Etna, Sicily, *Bull. Volcanol.*, *49*, 527–540.
- Guest, J. E., P. D. Spudis, R. Greeley, G. J. Taylor, and S. M. Baloga (1995), Emplacement of xenolith nodules in the Kaupulehu lava flow, Hualalai Volcano, Hawaii, *Bull. Volcanol.*, *57*, 179–184.
- Hiesinger, H., J. W. Head, and G. Neukum (2007), Young lava flows on the eastern flank of Ascraeus Mons: Rheological properties derived from High Resolution Stereo Camera (HRSC) images and Mars Orbiter Laser Altimeter (MOLA) data, *J. Geophys. Res.*, *112*, E05011, doi:10.1029/2006JE002717.
- Hodges, C. A., and J. H. Moore (1994), Atlas of volcanic landforms on Mars, *Prof. Pap. 1534*, 194 pp., U.S. Geol. Surv., Reston, Va.
- Hon, K., J. P. Kauahikaua, R. Denlinger, and K. Mackay (1994), Emplacement and inflation of pahoehoe sheet flows: Observations and measurements of active lava flows on Kilauea, Hawaii, *Geol. Soc. Am. Bull.*, *106*, 351–370.
- Hon, K., C. Gansecki, and J. Kauahikaua (2003), The transition from 'A'a to pahoehoe crust on flows emplaced during the Pu'u 'O'o-Kupaianaha eruption, in *The Pu'u 'O'o-Kupaianaha Eruption of Kilauea Volcano, Hawai'i: The First 20 Years*, edited by C. Heliker, D. A. Swanson, and T. J. Takahashi, *U.S. Geol. Surv. Prof. Pap.*, *1676*, 89–103.
- Hulme, G. (1974), The interpretation of lava flow morphology, *Geophys. J. R. Astron. Soc.*, *39*, 361–383.
- Leverington, D. W. (2004), Volcanic rilles, streamlined islands, and the origin of outflow channels on Mars, *J. Geophys. Res.*, *109*, E10011, doi:10.1029/2004JE002311.
- Lipman, P. W., and N. G. Banks (1987), AA flow dynamics, Mauna Loa 1984, in *Volcanism in Hawaii*, edited by R. W. Decker, T. L. Wright, and P. H. Stauffer, *U.S. Geol. Surv. Prof. Pap.*, *1350*, pp. 1527–1567.
- Malin, M. C. (1980), Lengths of Hawaiian lava flows, *Geology*, *8*, 306–308.
- Moore, M. J. (1987), Preliminary estimates of the rheological properties of 1984 Mauna Loa lava, in *Volcanism in Hawaii*, edited by R. W. Decker, T. L. Wright, and P. H. Stauffer, *U.S. Geol. Surv. Prof. Pap.*, *1350*, 1569–1588.
- Mougini-Mark, P., and M. T. Yoshioka (1998), The long lava flows of Elysium Planitia, Mars, *J. Geophys. Res.*, *103*(E8), 19,389–19,400.
- Nichols, R. L. (1936), Flow units in basalt, *J. Geol.*, *44*, 617–630.
- Peitersen, M. N., and D. A. Crown (1999), Downflow width behavior of Martian and terrestrial lava flows, *J. Geophys. Res.*, *104*(E4), 8473–8488.
- Peitersen, M. N., and D. A. Crown (2000), Correlations between topography and intraflow width behavior in Martian and terrestrial lava flows, *J. Geophys. Res.*, *105*(E2), 4123–4134.
- Pinkerton, H., and R. S. J. Sparks (1978), Field measurements of the rheology of lava, *Nature*, *276*, 383–384.
- Rowland, S. K., and G. P. L. Walker (1990), Pahoehoe and a'a in Hawaii: Volumetric flow rate controls the lava structure, *Bull. Volcanol.*, *52*, 615–628.
- Rowland, S. K., A. J. L. Harris, and H. Garbeil (2004), Effects of Martian conditions on numerically modeled, cooling-limited, channelized lava flows, *J. Geophys. Res.*, *109*, E10010, doi:10.1029/2004JE002288.
- Smith, D. E., et al. (1999), The global topography of Mars and implications for surface evolution, *Science*, *284*, 1495–1503.
- Theilig, E., and R. Greeley (1986), Lava flows on Mars: Analysis of small surface features and comparisons with terrestrial analogs, *Proc. Lunar Planet. Sci. Conf. 17th, Part I, J. Geophys. Res.*, *91*, suppl., E193–E206.

- Thordarson, T. (2000), Morphology and structure of the 1963–67 AD Surtsey lava flow field: Results from preliminary observations, *Surtsey Res.* 11, pp. 125–142, Surtsey Res. Soc., Reykjavik.
- Thordarson, T., and S. Self (1998), The Roza Member, Columbia River Basalt Group: A gigantic pahoehoe lava flow field formed by endogenous processes?, *J. Geophys. Res.*, 103(B11), 27,411–27,445.
- Walker, G. P. L. (1967), Thickness and viscosity of Etnean lava, *Nature*, 213, 484–485.
- Woodcock, D., and A. Harris (2006), The dynamics of a channel-fed lava flow on Pico Partido volcano, Lanzarote, *Bull. Volcanol.*, 69, 207–215.
- Zimelman, J. (1985), Estimates of rheologic properties for flows on the Martian volcano Ascraeus Mons, Proc. Lunar Planet. Sci. Conf. 16th, Part I, *J. Geophys. Res.*, 90, suppl., D157–D162.
-
- S. M. Baloga, Proxemy Research, 20528 Farcroft Lane, Gaithersburg, MD 20882, USA. (steve@proxemy.com)
- L. S. Glaze, NASA Goddard Space Flight Center, Code 698, Greenbelt, MD 20771, USA.